# High rates of sea-level rise during the last interglacial period

E. J. ROHLING[1]*, K. GRANT[1], CH. HEMLEBEN[2]*, M. SIDDALL[3], B. A. A. HOOGAKKER[4], M. BOLSHAW[1] AND M. KUCERA[2]

[1]National Oceanography Centre, European Way, Southampton SO45 5UH, UK
[2]Institute of Geosciences, University of Tübingen, Sigwartstrasse 10, 72076 Tübingen, Germany
[3]Lamont-Doherty Earth Observatory, 61 Route 9W - PO Box 1000, Palisades, New York 10964-8000, USA
[4]Department of Earth Sciences, University of Cambridge, Downing Street, Cambridge CB2 3EQ, UK
*e-mail: E.Rohling@noc.soton.ac.uk; christoph.hemleben@uni-tuebingen.de

Published online: 16 December 2007; doi:10.1038/ngeo.2007.28

**The last interglacial period, Marine Isotope Stage (MIS) 5e, was characterized by global mean surface temperatures that were at least 2 °C warmer than present[1]. Mean sea level stood 4–6 m higher than modern sea level[2–13], with an important contribution from a reduction of the Greenland ice sheet[1,14]. Although some fossil reef data indicate sea-level fluctuations of up to 10 m around the mean[3–9,11], so far it has not been possible to constrain the duration and rates of change of these shorter-term variations. Here, we use a combination of a continuous high-resolution sea-level record, based on the stable oxygen isotopes of planktonic foraminifera from the central Red Sea[15–18], and age constraints from coral data to estimate rates of sea-level change during MIS-5e. We find average rates of sea-level rise of 1.6 m per century. As global mean temperatures during MIS-5e were comparable to projections for future climate change under the influence of anthropogenic greenhouse-gas emissions[19,20], these observed rates of sea-level change inform the ongoing debate about high versus low rates of sea-level rise in the coming century[21,22].**

It is well established that past rates of sea-level rise due to ice-volume reduction have reached up to 5 m per century[23–25]. However, such values relate to deglaciations, dominated by disintegration of the now-absent Laurentide ice sheet, which questions their suitability for projections of future sea-level change within a well-developed interglacial period. So far, no detailed information exists about the rates of sea-level change associated with fluctuations within interglacial periods in general, and above 0 m in particular. This focuses attention on MIS-5e, the most recent (best dated) interglacial period during which sea level stood several metres above 0 m between roughly 124 and 119 kyr (thousand years ago) (see the Supplementary Information).

MIS-5e warmth was caused by orbital forcing of insolation, rather than the predicted greenhouse forcing of the near future, so that MIS-5e ice-volume responses may have differed in detail from future responses. However, we do not consider the MIS-5e warming as a straight analogy to the future, but instead aim to provide an observational context that quantifies the potential range of sea-level change rates above 0 m, to inform the debate about ice-volume reduction/sea-level rise in the next century that currently relies entirely on theoretical projections[21,22].

By dating fossil corals, previous studies have established that MIS-5e sea level reached an average highstand around +4 (±2) m, with individual maxima up to +7 or +9 m (refs 2–13) (see the Supplementary Information). Up to 5 m of this signal derived from reduction of the Greenland ice sheet[14]. There may also have been contributions from (West) Antarctica, which is responsive to climate change[26], although models suggest a slow and gradual response[22].

Although dated corals yield impressive insight into sea-level position and absolute age, they lack the tightly constrained relative-age framework needed to calculate rates of change. We overcome that problem by combining coral data with a new, continuous, highly resolved sea-level reconstruction through MIS-5e from the recent calibration method for central Red Sea stable oxygen isotope ($\delta^{18}O$) records[15–18], which offers tight stratigraphic control of relative ages.

Figure 1a shows new high-resolution $\delta^{18}O$ data from the MIS-6–5e deglaciation[15] through MIS-5e in central Red Sea sediment core GeoTü-KL11, superimposed on the previously published low-resolution record of KL11 for the entire MIS-6–4 interval[17,27] (see the Methods section). Also shown is a new 0.5–2-cm-resolution $\delta^{18}O$ record through MIS-5 from nearby core GeoTü-KL09, superimposed on a whole-core 10-cm-resolution record for that core (see the Methods section). Throughout this letter, records from cores KL11 and KL09 are correlated in the depth domain on the basis of simple linear matching between MIS-4 and the onset of MIS-5e, without any subjective 'fine-tuning' (Fig. 1a–d).

Figure 1b,d shows the $\delta^{18}O$ data converted into sea-level estimates, using the calibration developed for KL11 ($1\sigma = 6$ m) (see the Methods section)[15,17,18]. A first important observation is that sea level according to KL09 reached a shallowest value of about −17 m during MIS-5c, compared with about −40 m (or −30 m on the basis of low-resolution results of KL11) during MIS-5a (Fig. 1b). The MIS-5c value agrees with Barbados coral terraces, which suggest that sea level reached up to −16 m during both periods[28], but the MIS-5a value seems low relative to Barbados. We have yet to fully resolve MIS-5a, and consider our MIS-5c estimate more definitive than the MIS-5a value.

Figure 2 concentrates on MIS-5e in both KL11 and KL09, compared with a detailed series of coral-based sea-level estimates from Barbados[4]. The Red Sea results are shown versus depth in each core, and the KL11 series was calibrated to age by linearly matching

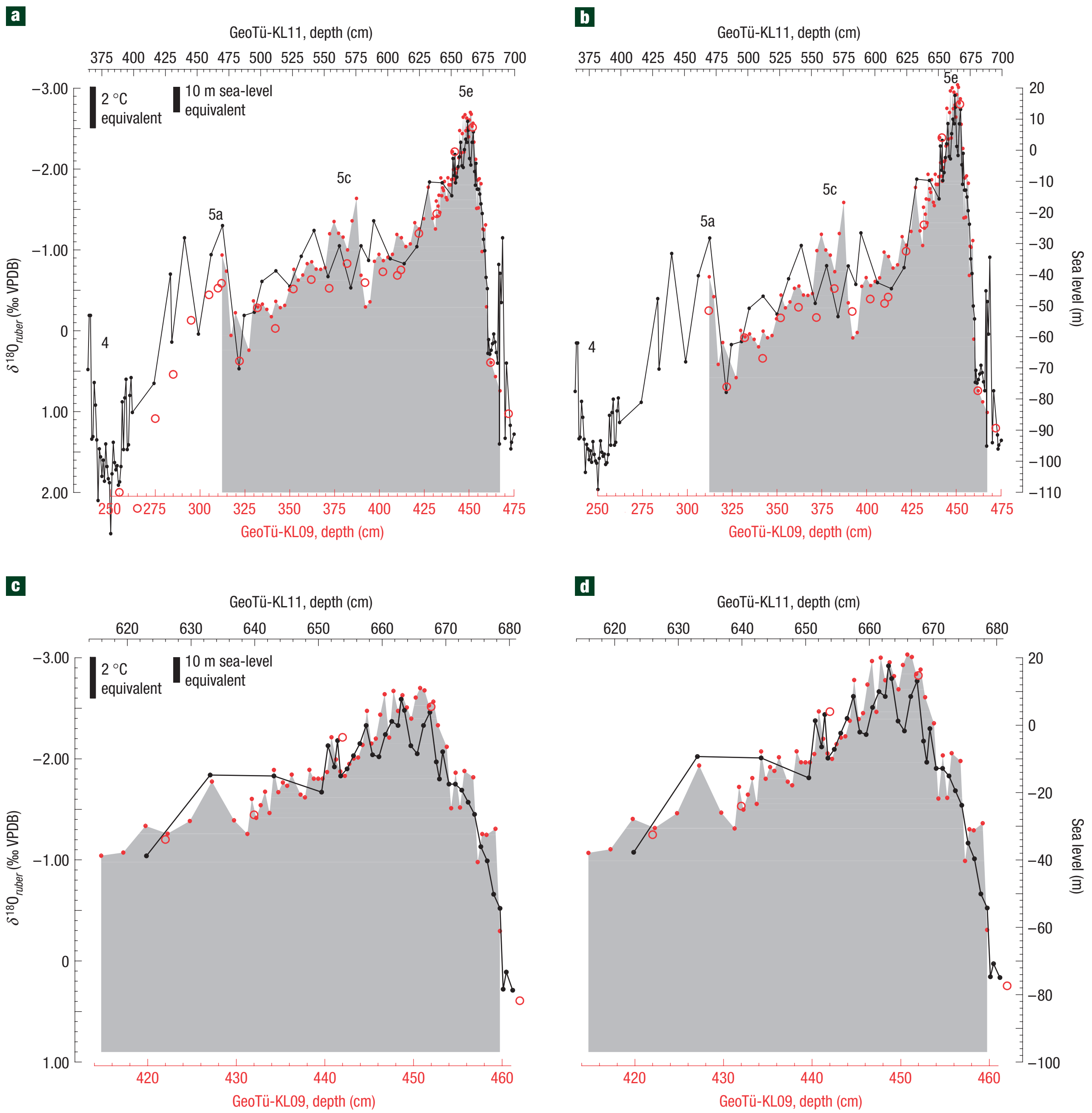


**Figure 1 Stable isotope and derived sea-level records for central Red Sea cores KL11 and KL09. a**, $\delta^{18}O_{ruber}$ throughout MIS-5e–4 for KL11 (black filled circles, line), alongside high-resolution data (red filled circles, grey shading) and a low-resolution series (red open circles) for KL09 (see the Methods section; VPDB: Vienna PeeDee Belemnite). Black bars indicate amplitudes of $\delta^{18}O$ change equivalent to about 2 °C temperature change and 10 m of sea-level change. The numbers identify Marine Isotope Stages. **b**, As **a**, but for sea level as derived from $\delta^{18}O_{ruber}$ (refs 17,18). **c**, As **a**, but magnified for a detailed comparison of trends within MIS-5e. **d**, As **c**, but for derived sea level.

the ‘inverted U’ shape of its long-term average sea-level trend to that in the dated corals[4] (Fig. 2a). Within MIS-5e, we maintain our straightforward linear KL11–KL09 correlation (Fig. 1a), so that the correlation of KL11 to the dated corals (Fig. 2a) implicitly yields an approximate age model for KL09 (Fig. 2b).

A 3,000 yr gaussian filter through KL11 reveals a long-term mean MIS-5e highstand up to +6 m, in agreement with the coral data (Fig. 2a). The same filter through KL09 reveals a comparable pattern (Fig. 2b) (see the Methods section). Shorter-term fluctuations are evaluated using a 750 yr filter through both records (Fig. 2c,d). Here, the two Red Sea records differ: the distinct fluctuations seen in KL11 are poorly/not represented in KL09 (Fig. 2c,d). Although this apparent discrepancy probably reflects different impacts of bioturbation in the two cores (see the Methods section), it does highlight a need for qualification of our results in terms of ‘robustness’. Accordingly, we first identify a detailed record of sea-level oscillations within MIS-5e on the basis of KL11, then investigate to what extent this record is supported by

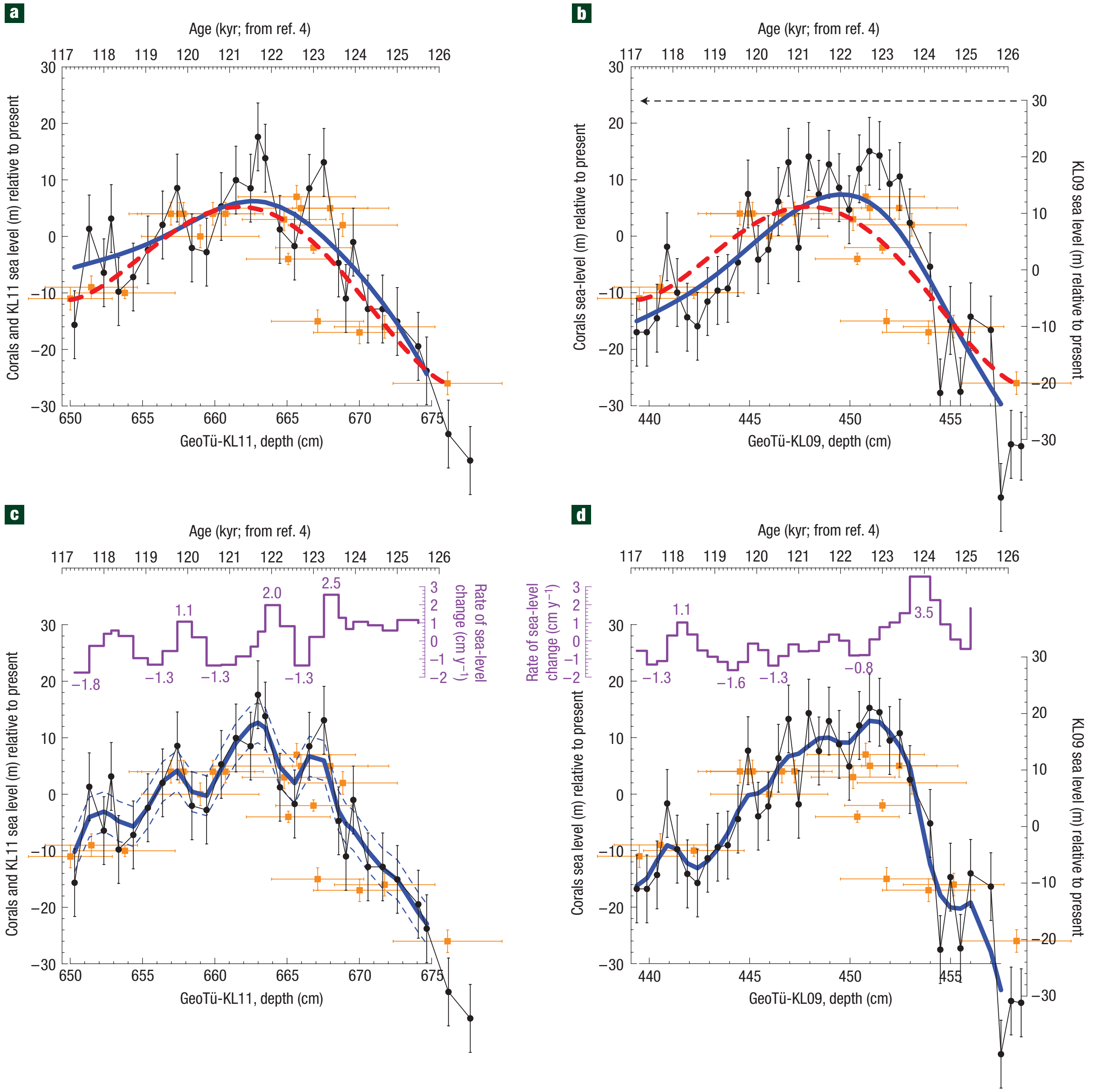


**Figure 2 MIS-5e high-resolution Red Sea sea-level reconstruction for KL11 and KL09 versus coral data.** KL11 and KL09: black lines/filled circles, $1\sigma = 6$ m error bars[17,18]; coral data: orange squares, with age/altitude error bars[4]. **a**, Long-term average trends: 3,000 year gaussian filter through KL11 (thick blue line); long-term trend in coral data (dashed red line). **b**, As **a**, for KL09. **c**, Short-term sea-level trends, from a 750 year gaussian filter through KL11 (thick blue line). Dashed blue lines show statistical 1 standard error for this record. The first time derivative of the thick blue record yields rates of change (purple step plot, with maximum rates of rise (positive) and lowering (negative)). **d**, As **c**, for KL09.

previous work, and finally identify which of the inferred features are most robust in that they are also obvious in KL09.

The $1\sigma = 6$ m uncertainty in the Red Sea sea-level method includes a ±1 °C uncertainty in sea surface temperature (SST) and a generous uncertainty for net evaporation[17,18]. To minimize the influence of any bias in individual points, we infer MIS-5e sea-level fluctuations after smoothing the data with a moving 750 yr gaussian filter (Fig. 2c). With $1\sigma = 6$ m for individual points, the standard error of the filtered mean sea-level record in KL11 is determined in a statistical sense for this particular data set (Monte Carlo method) at 1 standard error = 3.5 m (Fig. 2c). This yields the first sea-level record with the essential attributes (high temporal resolution and stratigraphic continuity) for quantification of rates of change associated with millennial-scale oscillations within MIS-5e. First, however, we consider whether there is support from other, independent sea-level indicators for the inferred oscillations (Fig. 2c). Ages reported for the Red Sea record are subject to the about ±1 kyr uncertainty margin of the coral datings that underlie our age model[4] (Fig. 2a). However, the tightly constrained stratigraphic order of our records stipulates that such age uncertainties will be systematically distributed along the record, so that age uncertainties are much smaller than ±1 kyr where relative sample ages (hence, durations) are concerned.

Although some studies of MIS-5e corals favour a single highstand rather than a compound structure[2,3,13], there is a hiatus in the Western Australian record[3] that may agree with suggestions of intra-MIS-5e sea-level instability around 122 ± 1 kyr in fossil reef records from Barbados[4], the Bahamas[3,8,9] and the Red Sea[5–7,11,12] (see Supplementary Information, Table S1). KL11 suggests two main highstands around 123 and 121.5 kyr, separated by a relative lowstand around 122.5 kyr (Fig. 2c). A third minor highstand is suggested around 119.5 kyr, after a relative lowstand centred on 120.5 kyr. The amplitude of the latter fluctuation, as well as that of the sea-level drop following the 119.5 kyr high, is well supported by the coral data[4] (Fig. 2c). The same holds for the early MIS-5e rise into the first highstand of 123 kyr (Fig. 2c), and it was previously found that detailed sea-level fluctuations inferred from the Red Sea record for the MIS-6 to 5e deglaciation agree with independent coral and speleothem data[15]. Furthermore, we note that the coral-based sea-level estimates[4] may be suggestive of a sea-level fluctuation of similar amplitude to our inferred sea-level drop around 122.5 kyr (Fig. 2c). The second MIS-5e highstand inferred from the Red Sea record (∼121.5 kyr) resides within a conspicuous gap in the Barbados data[4], but similar work around the Gulf of Aqaba reports terraces up to +10 m that date to 121–122 kyr (ref. 29).

Despite some apparent agreements, the lack of temporal resolution and stratigraphic continuity clearly limits the use of dated coral series for comprehensive validation of our record's finer structure. In addition, the validity of detailed time-series comparisons (as above) might be questioned, given the dating uncertainties. Finally, it has been suggested that rapid sea-level fluctuations may not be represented by well-developed corals[30]. Detailed stratigraphic descriptions of reef/coastal architecture sequences may help, as they yield better insight into the temporal sequence of events.

Such work along the Egyptian coast of the northern Red Sea reveals two main highstand peaks (around +5 to +9 m), separated by a brief 7–10 m sea-level drop[5–7] (see Supplementary Information, Fig. S1). The absolute altitude of the deposits might be affected by uplift, but due to its gradual/long-term nature, uplift cannot account for the centennial-scale relative sequence of two peaks separated by a sharp drop, or for the amplitude of the fluctuations. Note that Red Sea sea-level records based on fossil reefs and coastal deposits[5–7,10–12] are conceptually, technically and tectonically independent from our reconstructions. The reef/coastal sequences[5–7] thus offer strong independent support to the main intra-MIS-5e sea-level fluctuation suggested by our record, with two main highstands (123 and 121.5 kyr) separated by a sharp drop (122.5 kyr) (Fig. 2c). Even the inferred amplitudes of change agree.

Reef-architecture studies on the Eritrean coast of the southern Red Sea[11,12] seem to corroborate not only the two main highstands in our record, but even the minor third peak[11] (Fig. 2c). Although only qualitatively described, the work identifies an initial rapid sea-level rise (their subunit $5e_1$), a drop, a second sea-level rise ($5e_2$), another minor drop, and finally a minor peak with patch reef development ($5e_3$) before the final drop at the end of MIS-5e[11] (see Supplementary Information, Fig. S2). The various reef/coastal sequence studies describe the intra-MIS-5e sea-level drop(s) as erosive/consolidation phases without apparent new reef formation[5–7,11]. Such transient events would probably be missed in time series of dated corals.

Both the structure and amplitude of our KL11 record of MIS-5e sea level (Fig. 2c) are therefore empirically validated (within error margins) by four main observations. These are: the general consensus that sea level reached a longer-term mean position up to +6 m; the observations of individual (peak) deposits up to about +9 m; the suggestions of intra-MIS-5e sea-level variability in a variety of records; and the agreement between our reconstruction and detailed reef/coastal architecture studies regarding the sequence of events within MIS-5e. Moreover, our reconstruction is robust with respect to sedimentation rate within KL11, isostatic effects and regional fluctuations in temperature and net evaporation (see the Supplementary Information).

We now use our record to estimate the rates of MIS-5e sea-level rise. The first time derivative of the short-term smoothed KL11 record shows peak rates of rise of 2.5, 2.0 and 1.1 m per century (Fig. 2c). Mean coral values suggest comparable rates of rise of 1.7 and 1.0 m per century through the intervals 124.7–123.3 and 120.5–119.8 kyr, respectively (Fig. 2). Because overall chronology is critical to the derived rates of sea-level rise, we derive a representative maximum duration for the MIS-5e highstand above 0 m from the literature (see Supplementary Information, Table S1). On the basis of an age range of about 119–128 kyr, this maximum duration is about twice that indicated in Fig. 2. This conservative way of assessing uncertainty in the rates of sea-level rise yields the very minimum estimates for the rates of MIS-5e sea-level rise, being 1.3, 1.0 and 0.6 m per century. We thus infer a full potential range for the rates of rise between 2.5 and 0.6 m per century. We also note that sea-level lowering events reveal a remarkably consistent rate between −1.3 and −1.8 (−0.7 to −0.9) m per century (values in brackets refer to a doubled MIS-5e duration).

Although the intra-MIS-5e oscillations in KL11 seem to be corroborated by coral and reef architecture data, we consider them as only strongly suggestive, because they are not fully replicated in KL09 (see the Methods section). However, two events are common to both records and consequently seem particularly robust (Fig. 2c,d). These are the rise above 0 m at the onset of MIS-5e around 123.5 kyr and the drop ending the main highstand around 119 kyr. The rate of rise above 0 m around 123.5 kyr is 1.5–2.5 (0.8–1.3) m per century, whereas the rate of lowering around 119 kyr is −1.3 to −1.6 (−0.7 to −0.8) m per century. On the basis of only these robust events, therefore, the rate of rise above 0 m from the Red Sea data would be 1.6 ± 0.8, similar to the 1.6 ± 1.0 m per century estimate based on all MIS-5e fluctuations in KL11.

A 1.6 m global sea-level rise per century would correspond to disappearance of an ice sheet the size of Greenland in roughly four centuries (modelling suggests 1,000 years or more[20]). During MIS-5e, such rates of sea-level rise occurred when the global mean temperature was 2 °C higher than today, as expected again by AD 2100 (refs 19,20,22). Using MIS-5e to gain insight into the potential rates of sea-level rise due to further ice-volume reduction in a warming world, our data provide an observational context that underscores the plausibility of recent, unconventionally high, projections of 1.0 ± 0.5 m sea-level rise by AD 2100 (ref. 21).

## METHODS

We present stable isotope data for the surface-water dwelling planktonic foraminiferal species *Globigerinoides ruber* (white) in two central Red Sea sediment cores: GeoTü-KL11 (18° 44.5′ N, 39° 20.6′ E, 825 m waterdepth) and GeoTü-KL09 (19° 57.6′ N, 38° 08.3′ E, 814 m waterdepth), which we refer to in abbreviated form as KL11 and KL09. Samples for KL11 were prepared in Tübingen and analysed in Kiel, Germany, on a MAT251 mass spectrometer, over the period 1988–1996. For KL09, a low-resolution pilot series of samples was prepared in Tübingen and analysed in Southampton on a Europa Geo2020 mass spectrometer, in 2006. The high-resolution series for KL09 was prepared and analysed in 2006–2007 in Southampton, using the Geo2020. Each analysis represents a set of at least 10 and usually more than 20 specimens, and external precision ($1\sigma$) is 0.06%. Despite the different equipment, lab protocols, operators and sampling and preparation methods in the two separate sediment cores, the records of KL09 and KL11 agree well, especially when allowing for the external precision (Fig. 1a).

Calibration of $\delta^{18}O_{ruber}$ variations in KL11 into sea-level change is described in detail in refs 15,17,18. The scaling used in that method infers a regional mean annual MIS-5e SST that is up to 0.5 °C warmer than the present (±1 °C at the $1\sigma$ level), which is within the range suggested by alkenone-based reconstructions for the nearby easternmost Mediterranean[31]. An extensive pilot study of MIS-5e SST in KL09 is discussed in the Supplementary Information. Calibration of KL09 $\delta^{18}O_{ruber}$ to sea level was done using the calibration method developed for KL11 (refs 15,17,18). It may be expected, however, that absolute $\delta^{18}O_{ruber}$ values at different sites may be offset from one another (for example, as a function of latitude within the basin[16,18] or temperature differences between sites). We use the mean long-term sea-level trend in KL09 in comparison with the coral data to compensate for the potential artefact that was introduced when calibrating KL09 data using the KL11-specific calibration between $\delta^{18}O_{ruber}$ and sea level. A reasonable fit is found when shifting inferred KL09 sea-level values down by about 6 m (Fig. 2b, dashed arrow). As the $1\sigma$ margin of the sea-level calibration is about 6 m (refs 17,18), this inferred offset remains comfortably within the overlapping $1\sigma$ bands around the KL11 and KL09 sea-level reconstructions. In terms of $\delta^{18}O$, the inferred 6 m offset would imply that KL11 $\delta^{18}O_{ruber}$ is systematically about 0.2% heavier than contemporaneous KL09 $\delta^{18}O_{ruber}$, which would be equivalent to less than 1 °C temperature difference between the sites.

We attribute the difference between the shorter-term fluctuations apparent within MIS-5e in KL11 and KL09 (Fig. 2c,d) to different impacts of bioturbation in the two cores. Sediment accumulation rates through MIS-5e are about 1.5 times higher in KL11 than in KL09 (compare depth axes in Figs 1, 2). As KL11 was sampled in 1 cm steps and KL09 in 0.5 cm steps, the resultant temporal resolution might seem better in KL09 than in KL11 (Fig. 2), but the low-pass filtering effect of bioturbation during sediment accumulation would cause considerable smoothing of high-frequency signals in lower accumulation settings (KL09), whereas these may be preserved under higher accumulation conditions (KL11).

Received 1 May 2007; accepted 11 October 2007; published 16 December 2007.

## References


1. Otto-Bliesner, B. L. *et al*. Simulating Arctic climate warmth and icefield retreat in the last interglaciation. *Science* **311**, 1751–1753 (2006).
2. McCulloch, M. T. & Esat, T. The coral record of last interglacial sea levels and sea surface temperatures. *Chem. Geol.* **169**, 107–129 (2000).
3. Stirling, C. H., Esat, T. M., Lambeck, K. & McCulloch, M. T. Timing and duration of the Last Interglacial: Evidence for a restricted interval of widespread coral reef growth. *Earth Planet. Sci. Lett.* **160**, 745–762 (1998).
4. Thompson, W. G. & Goldstein, S. L. Open-system coral ages reveal persistent suborbital sea-level cycles. *Science* **308**, 401–404 (2005).
5. Plaziat, J. C. *et al.* Mise en evidence, sur la côte récifale d'Egypte, d'une régression interrompant le plus haut niveau du Dernier Interglaciaire (5e): Un nouvel indice de variations glacio-eustatiques haute fréquence au Pléistocène? *Bull. Soc. Geol. Fr.* **169**, 115–125 (1998).
6. Plaziat, J. C. *et al.* Quaternary changes in the Egyptian shoreline of the northwestern Red Sea and Gulf of Suez. *Quat. Internat.* **29/30**, 11–22 (1995).
7. Orszag-Sperber, F., Plaziat, J. C., Baltzer, F. & Purser, B. H. Gypsum salina-coral reef relationships during the Last Interglacial (Marine Isotopic Stage 5e) on the Egyptian Red Sea coast: A Quaternary analogue for Neogene marginal evaporites? *Sedim. Geol.* **140**, 61–85 (2001).
8. Neumann, A. C. & Hearty, P. J. Rapid sea-level changes at the close of the last interglacial (substage 5e) recorded in Bahamian island geology. *Geology* **24**, 775–778 (1996).
9. Chen, J. H., Curran, H. A., White, R. & Wasserburg, G. J. Precise chronology of the last interglacial period: $^{234}U$–$^{230}Th$ data from fossil coral reefs in the Bahamas. *Geol. Soc. Am. Bull.* **103**, 82–97 (1991).
10. El-Asmar, H. M. Quaternary isotope stratigraphy and paleoclimate of coral reef terraces, Gulf of Aqaba, South Sinai, Egypt. *Quat. Sci. Rev.* **16**, 911–924 (1997).
11. Bruggemann, J. H. *et al*. Stratigraphy, palaeoenvironments and model for the deposition of the Abdur Reef Limestone: Context for an important archaeological site from the last interglacial on the Red Sea coast of Eritrea. *Palaeogeogr. Palaeoclimatol. Palaeoecol.* **203**, 179–206 (2004).
12. Walter, R. C. *et al*. Early human occupation of the Red Sea coast of Eritrea during the last interglacial. *Nature* **405**, 65–69 (2000).
13. Stirling, C. H., Esat, T. M., McCulloch, M. T. & Lambeck, K. High-precision U-series dating of corals from Western Australia and implications for the timing and duration of the Last Interglacial. *Earth Planet. Sci. Lett.* **135**, 115–130 (1995).
14. Cuffey, K. M. & Marshall, S. J. Substantial contribution to sea-level rise during the last interglacial from the Greenland ice sheet. *Nature* **404**, 591–594 (2000).
15. Siddall, M., Bard, E., Rohling, E. J. & Hemleben, Ch. Sea-level reversal during Termination II. *Geology* **34**, 817–820 (2006).
16. Arz, H. W. *et al*. Dominant Northern Hemisphere climate control over millennial-scale glacial sea-level variability. *Quat. Sci. Rev.* **26**, 312–321 (2007).
17. Siddall, M. *et al*. Sea-level fluctuations during the last glacial cycle. *Nature* **423**, 853–858 (2003).
18. Siddall, M. *et al*. Understanding the Red Sea response to sea level. *Earth Planet. Sci. Lett.* **225**, 421–434 (2004).
19. Folland, C. K. *et al*. in *Climate Change 2001, The Scientific Basis. Contribution of Working Group I to the Third Assessment Report of the Intergovernmental Panel on Climate Change* (ed. Houghton, J. T. *et al.*) 99–181 (Cambridge Univ. Press, Cambridge and New York, 2001).
20. Gregory, J. M., Huybrechts, P. & Raper, S. C. B. Threatened loss of the Greenland ice sheet. *Nature* **428**, 616 (2004).
21. Rahmstorf, S. A semi-empirical approach to projecting future sea-level rise. *Science* **315**, 368–370 (2007).
22. Church, J. M. *et al*. in *Climate Change 2001, The Scientific Basis. Contribution of Working Group I to the Third Assessment Report of the Intergovernmental Panel on Climate Change* (ed. Houghton, J. T. *et al.*) 639–693 (Cambridge Univ. Press, Cambridge and New York, 2001).
23. Fairbanks, R. G. A 17,000-year glacio-eustatic sea level record: Influence of glacial melting rates on the Younger Dryas event and deep-ocean circulation. *Nature* **342**, 637–642 (1989).
24. Blanchon, P. & Shaw, J. Reef drowning during the last deglaciation: Evidence for catastrophic sea-level rise and ice-sheet collapse. *Geology* **23**, 4–8 (1995).
25. Stanford, J. D. *et al*. Timing of meltwater pulse 1a and climate responses to meltwater injections. *Paleoceanography* **21**, PA4103 (2006).
26. Cazenave, A. How fast are the ice sheets melting? *Science* **314**, 1250–1252 (2006).
27. Hemleben, Ch. *et al*. Three hundred and eighty thousand year-long stable isotope and faunal records from the Red Sea. *Paleoceanography* **11**, 147–156 (1996).
28. Schellmann, G. & Radtke, U. A revised morpho- and chronostratigraphy of the late and middle Pleistocene coral reef terraces on Southern Barbados (West Indies). *Earth Sci. Rev.* **64**, 157–187 (2004).
29. Scholz, A., Mangini, A. & Felis, T. U-series dating of diagenetically altered fossil reef corals. *Earth Planet. Sci. Lett.* **218**, 163–178 (2004).
30. Hearty, P. J., Neumann, A. C. & O'Leary, M. J. Comment on 'Record of MIS5 sea-level highstands based on U/Th dated coral terraces of Haiti' by Dumas *et al.* [Quaternary International 2006 106–118]. *Quat. Internat.* **162/163**, 205–208 (2007).
31. Rohling, E. J. *et al*. African monsoon variability during the previous interglacial maximum. *Earth Planet. Sci. Lett.* **202**, 61–75 (2002).


## Acknowledgements

We thank all colleagues who have offered advice that helped shape the arguments in this manuscript, I. Schmeltzer, S. Geiselhart and H. Erlenkeuser for work on core KL11, and G. Trommer and M. Siccha for work on KL09. H. Elderfield provided valuable feedback to the Mg/Ca pilot study, and I. Marshall and C. Hayward helped with scanning electron microscope and electron microprobe analyses. This study was supported by the UK Natural Environment Research Council (NERC, NE/C003152/1), the German Science Foundation (DFG, He 697/17; Ku 2259/3) and EC project STOPFEN (HPRN-CT-2002-00221).
Correspondence and requests for materials should be addressed to E.J.R. or Ch.H.
Supplementary Information accompanies this paper on www.nature.com/naturegeoscience.

Reprints and permission information is available online at http://npg.nature.com/reprintsandpermissions/